ORIGINAL ARTICLE

Selection Moment Invariants Feature Extraction Techniques of Medical Images Based on Intraclass Analysis

Mohd Wafi Nasrudin[1], Nur Diana Mastura Zulkifli[2], Wan Azani Mustafa[3], Rashidah Che Yob[4], Norfatihah Bahari[4]

[1] Advanced Computing, Centre of Excellence (CoE), Faculty of Electronic Engineering Technology, Campus Pauh Putra, Universiti Malaysia Perlis, 02600 Arau, Perlis, Malaysia
[2] Department of Pathology, Hospital Tuanku Fauziah, 01000 Kangar, Perlis, Malaysia.
[3] Faculty of Electric Engineering & Technology, Campus Pauh Putra, Universiti Malaysia Perlis, 02600 Arau, Perlis, Malaysia.
[4] Faculty of Electronic Engineering & Technology, Campus Pauh Putra, Universiti Malaysia Perlis, 02600 Arau, Perlis, Malaysia.

ABSTRACT

Introduction: Medical imaging plays a vital role in clinical diagnostics, yet geometric distortions such as rotation, translation, and scaling can reduce the accuracy of computer-aided diagnostic (CAD) systems. Moment invariants are widely applied in feature extraction because of their mathematical robustness against such transformations. Among the many orthogonal moment families (Zernike, Pseudo-Zernike, Hahn, Tchebichef, etc.), this study focuses on Legendre Moment Invariants (LMI) and Krawtchouk Moment Invariants (KMI) as representatives of global versus local approaches. A subset of images from the COVID-19 Radiography Database was used, with inclusion restricted to clear frontal chest X-rays. Controlled geometric transformations rotation, scaling, and combined distortions were applied. Feature vectors were extracted using LMI and KMI, and their performance was evaluated via intraclass analysis using Absolute Error (AE), Percentage Absolute Error (PAE), Percentage Mean Absolute Error (PMAE), and Total Percentage Mean Absolute Error (TPMAE). Analysis was conducted in MATLAB R2023a. Both methods demonstrated invariance properties; however, KMI consistently achieved lower AE, PAE, and TPMAE values across transformation conditions. This suggests that its discrete and localized representation preserves features more effectively than LMI, which exhibited higher sensitivity to scaling and combined distortions. Findings indicate that KMI offers superior robustness for medical image feature extraction under geometric variations, making it a promising candidate for CAD systems. Nonetheless, this study is limited by its small dataset and scope. It should be regarded as a proof-of-concept, with future work required to expand the evaluation to larger datasets, additional moment invariant families, and statistical validation.
Malaysian Journal of Medicine and Health Sciences (2025) 21(SUPP11): 75-81.doi:10.47836/mjmhs.21.s11.11

Keywords: Legendre moment invariants, Krawtchouk moment invariants, Medical image, Shape analysis, Intra-class analysis

Corresponding Author:
Mohd Wafi Nasrudin, PhD
Email : wafi@unimap.edu.my
Tel : 04-9885509

INTRODUCTION

Feature extraction is a fundamental step in pattern recognition and medical image analysis. The aim is to derive numerical descriptors that can reliably distinguish one object from another while remaining stable under variations such as rotation, translation, and scaling. Among the many available techniques, moment invariants have been widely applied due to their strong mathematical foundation and robustness against geometric transformations (1,2).

Over the years, numerous families of orthogonal polynomials have been proposed, including Zernike, Pseudo-Zernike, Hahn, Tchebichef, Legendre, and Krawtchouk moments. Each of these methods offers a different trade-off between global and local feature representation, computational complexity, and sensitivity to distortions. Comparative studies are therefore valuable in understanding their relative strengths and limitations.

This study focuses specifically on Legendre Moment Invariants (LMI) and Krawtchouk Moment Invariants (KMI). The rationale for selecting these two techniques lies in their distinct characteristics: LMI, introduced in 1980 (Teague (3), represents a continuous, global moment family, whereas KMI (Yap (4) is based on discrete, localized polynomials that enable finer feature preservation. Several practical applications have highlighted their potential: Legendre moments have been used in copy–move forgery detection (5), vehicle logo recognition (6), and symmetry-based image reconstruction (7). Krawtchouk moments, on the other hand, have been successfully applied to limited-view CT reconstruction (8), 3D objects recognition (9), and sign language recognition using quaternion algebra (10). These applications demonstrate the versatility of both moment families across diverse domains.

In the context of medical imaging, protocols typically minimize extreme distortions; however, variations still occur due to patient positioning, equipment calibration, and image resolution differences. Such geometric inconsistencies, even when subtle, may reduce the robustness of computer-aided diagnostic (CAD) systems. Consequently, evaluating the relative performance of global versus local invariant techniques on medical images is clinically relevant.

The present work applies intraclass analysis to compare LMI and KMI under controlled geometric distortions, including rotation, scaling, and combined transformations. Intraclass analysis refers to the process of analyzing differences between the original image and a new set of images with varying rotation and scale factors. This analysis is computed using feature vectors produced by Moment Invariant techniques, which represent the shape features of images. A series of equations are used to identify the best technique by measuring similarities between these feature vectors (11,12). Intraclass analysis quantifies stability through metrics such as Absolute Error (AE), Percentage Absolute Error (PAE), Percentage Mean Absolute Error (PMAE), and Total Percentage Mean Absolute Error (TPMAE). A technique is considered optimal when TPMAE values remain small across distortions (13, 14).

The contributions of this study are threefold:

1. A comparative evaluation of LMI and KMI on chest radiography images subjected to geometric distortions.
2. A rigorous performance assessment using intraclass analysis metrics.
3. A discussion of the implications of the findings for robust medical image feature extraction, along with limitations and directions for future work.

This study is intended as a proof-of-concept, providing a foundation for broader comparative analyses across multiple datasets and moment invariant families.

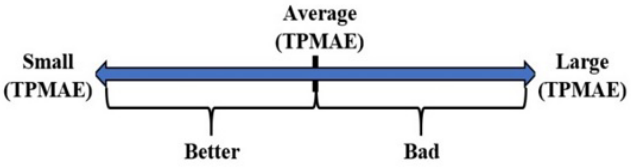

Figure 1: Depiction of the intra-class. This figure illustrates the performance measurement criteria for the Moment Invariants technique. It shows that a lower Total Percentage Mean Absolute Error (TPMAE) indicates a better-performing technique, while a higher TPMAE suggests less effectiveness.

MATERIALS AND METHODS

Dataset and Image Selection

This study used images from the COVID-19 Radiography Database, a publicly available dataset. Inclusion criteria required clear, standard-quality frontal chest radiographs. Lateral views and poor-quality images were excluded. For this proof-of-concept study, a representative chest X-ray was selected to demonstrate the methodology.

Moment Invariants Framework

Two types of moment invariants were implemented in this study, namely Legendre Moment Invariants (LMI) and Krawtchouk Moment Invariants (KMI). Both methods were evaluated for their effectiveness in extracting stable feature vectors from medical images when subjected to geometric transformations such as rotation, scaling, and their combination.

Legendre Moment Invariants

LMI is derived from Legendre polynomials. The Legendre moment of order (p+q) can be expressed in terms of geometric moments using Equations (1) and (2). To achieve invariance to translation, rotation, and scaling, the formulation in Equation (1) is adjusted as in Equation (3), where normalization and rotation factors are included:

$$L_{pq} = \frac{(2p+1)(2q+1)}{4} \sum_{i=0}^{p} \sum_{i=0}^{q} a_{pi}\, a_{qj}\, v_{ij} \quad (1)$$

$$a_{pi} = P_n(\chi) = \sum_{k=0}^{n} (-1)^{(n-k)/2} \frac{1}{2^n} \frac{(n+k)!\,\chi^k}{\left(\frac{n-k}{2}\right)!\ \left(\frac{n+k}{2}\right)!k!} \quad (2)$$

$$v_{nm} = m^{\gamma}_{00} \sum_{\chi=1}^{N} \sum_{y=1}^{M} [\chi - \tilde{\chi}) \cos\theta + (y - \tilde{y}) \sin\theta]^n X\ [(y - \tilde{y})\ \cos\theta - (\chi - \tilde{\chi})\ \sin\theta]^m f(x, y) \quad (3)$$

Where:

$$\theta = \frac{1}{2} \tan^{-1} \frac{2\mu_{11}}{\mu_{20} - \mu_{02}} \quad (4)$$

$$\gamma = \frac{n+m}{2} + 1 \quad (5)$$

where:

- (p,q) are the moment orders,
- γ is the normalization factor for scale invariance,
- θ is the rotation adjustment parameter,
- (x,y) are pixel coordinates, and
- f(x,y) is the image intensity at location (x,y).

Equations (4) and (5) compute γ and θ, respectively.

Krawtchouk Moment Invariants

KMI is based on discrete orthogonal Krawtchouk polynomials and is formulated as linear combinations of geometric moments. The general expression of KMI for order (n+m) is defined in Equations (6) to (11). Equation (12) defines the recursive computation of the polynomial basis functions. These discrete formulations allow KMI to capture localized image features more effectively than global moments such as LMI.

$$K_{nm} = \Omega_{nm} \sum_{i=0}^{n} \sum_{j=0}^{m} a_{i,n,p1}\, a_{j,m,p2}\, \tilde{v}_{ij} \tag{6}$$

$$\Omega_{nm} = [\, \rho(n; p_1, N-1)\, \rho(n; p_2, N-1)\,]^{-0.5} \tag{7}$$

$$\rho(n; p, N) = (-1)^n \left[\frac{1-p}{p}\right]^n \frac{n!}{(-N)_n} \tag{8}$$

$$K_n(\chi; p, N) = \sum_{k=0}^{n} a_{k,n,p}\, \chi^k = {}_2F_1\left[-n, -\chi; -N; \frac{1}{p}\right] \tag{9}$$

$$\tilde{v}_{ij} = \sum_{p=0}^{i} \sum_{q=0}^{j} \binom{i}{p} \binom{j}{q} \binom{N^2}{2}^{\frac{p+q}{2}+1} \binom{N}{2}^{i+j-p-q} v_{pq} \tag{10}$$

$${}_2F_1\left[-n, -\chi; -N; \frac{1}{p}\right] = \sum_{k=0}^{n} \frac{(-n)_k\, (-\chi)_k}{(-N)_k} \times \frac{(p)^{-k}}{k!} \tag{11}$$

The computation of $(x)_n$ for n = 0,1,2, … are given as follows:

$$(\chi)_0 = 1$$
$$(\chi)_1 = \chi$$
$$(\chi)_2 = \chi^2 + \chi$$
$$(\chi)_3 = \chi^3 + 3\chi^2 + 2\chi$$
$$(\chi)_4 = \chi^4 + 6\chi^3 + 11\chi^2 + 6\chi \tag{12}$$

Experimental

For this study, a representative chest X-ray image from the COVID-19 Radiography Database (Figure 2) was used to evaluate the invariance properties of the two techniques. The image was subjected to controlled geometric transformations to simulate real-world distortions:

•Rotation invariance: images rotated at multiple angles.
•Scale invariance: scaling at factors of 0.4, 0.6, and 0.8.
•Combined invariance: simultaneous application of rotation and scaling.

Figure 2: Chest X-ray. Chest X-ray image used in the study. This image is sourced from the COVID-19 Radiography Database and serves as the sample medical image for evaluating the invariance properties of the moment invariants techniques.

For each transformation condition, feature vectors were extracted using both Legendre Moment Invariants (LMI) and Krawtchouk Moment Invariants (KMI). These vectors were then analyzed using intraclass metrics to assess the robustness of each method.

Intraclass Analysis

To determine which technique yields the most stable results, an intraclass analysis was performed to compare LMI and KMI under rotation, scaling, and combined transformations. This analysis quantifies the similarity of feature vectors extracted from the original and transformed images. The intraclass analysis will be computed using the following series of equations:

$$AE_{im}^{a}\gamma_i = \Delta_m^a \gamma_i = |\, H_a(\gamma_i) - F_m^a(\gamma_i)\, | \tag{13}$$

$$PAE_{im}^{a}(\gamma_i) = \%\Delta_m^a \gamma_i = \frac{\Delta_m^a \gamma_i}{|\, H_a(\gamma_i)\, |} \times 100 \tag{14}$$

$$PMAE_{m}^{a}(\gamma) = \frac{1}{I} \sum_{i=1}^{I} PAE_{im}^{a}(\gamma_i) \tag{15}$$

$$TPMAE_a = \frac{1}{M} \sum_{m=1}^{M} PMAE_{m}^{a}(\gamma) \tag{16}$$

Based on the equations for intraclass analysis, the first step is to compute the absolute error using Equation (13). Next, the Percentage of Absolute Error is determined using Equation (14). Then, the Percentage Mean Absolute Error is obtained using Equation (15). Finally, the Total Percentage Mean Absolute Error (TPMAE) for the image class in each dimension is calculated using Equation (16).

RESULTS

Feature Vector Analysis

The feature vectors generated by the Moment Invariants techniques are shown in Tables 1 and 2. These feature vectors represent six elements (Ø1 to Ø6) and are recorded under different conditions such as rotation angles (5°, 10°, 15°, etc.) and scaling factors (0.4, 0.6, 0.8). Each technique yields distinct values, reflecting the impact of different transformations on feature stability. In Table 1, Krawtchouk Moment Invariants (KMI) feature vectors display relatively stable values across increasing rotation angles. Similarly, scaling factors show moderate deviations, confirming the theoretical robustness of KMI against geometric changes. Conversely, Table 2 presents the Legendre Moment Invariants (LMI) feature vectors, which exhibit higher sensitivity to transformations, particularly under combined rotation and scaling distortions.

Table I. Krawtchouk Moment Invariant Feature Vector

Image variation	Ø1	Ø2	Ø3	Ø4	Ø5	Ø6
Original	5.6775268	5.58566285	7.9495430	7.90360992	7.75690395	7.61910448
5	5.5833403	5.60151647	7.8632806	7.87236902	7.61561821	7.64288323
10	5.5819516	5.594832559	7.8585532	7.86499395	7.61353829	7.63286027
15	5.6742627	5.71484073	8.0108640	8.03115347	7.75200549	7.81287387
20	5.6871351	5.56915483	7.9509022	7.89191059	7.77132139	7.59434631
25	5.6278177	5.55340069	7.8837007	7.84649121	7.68233598	7.57070730
30	5.6058156	5.55808085	7.8640405	7.84017246	7.64933392	7.57772963
35	5.5927786	5.56335432	7.8536449	7.83893240	7.62978266	7.58564492
40	5.5832678	5.56899735	7.8469516	7.83981613	7.61551209	7.59410567
45	5.5754057	5.57500724	7.8422887	7.84208952	7.60391301	7.60331526
0.4	6.0849678	5.99971217	8.2660717	8.27344411	8.12012544	8.24224258
0.6	5.8232606	5.86452238	8.3128577	8.23348918	8.05365254	8.11554687
0.8	5.7208898	5.67128531	8.0888060	8.06400308	7.87503533	7.80062647
0.4+25	6.1239175	6.04947802	8.2799145	8.34269376	8.17856103	8.26689862
0.4+45	6.1721581	6.17222584	8.3339124	8.33915788	8.10051515	8.20061671
0.8+25	5.8215840	5.74733337	8.0775236	8.04039723	7.87607562	7.76469651
0.8+45	5.7694153	5.76911266	8.0363357	8.03618432	7.79791205	7.79745794

Table II. Legendre Moment Invariant Feature Vector

Image variation	Ø1	Ø2	Ø3	Ø4	Ø5	Ø6
Original	2.21650426	2.77698028	3.57814424	-2.99351500	-1.39965593	1.52805864
5	2.21703951	2.77662532	3.61637119	2.92935639	1.33614845	1.56555298
10	2.21707827	2.77676349	3.59900239	2.92683659	1.33351274	1.54822284
15	2.21644909	2.77755105	-3.54425687	-3.00666989	-1.41220887	-1.4945417
20	2.21669962	2.77745815	3.54905131	-2.9628929	-1.36866548	1.49903600
25	2.21627459	2.77800598	3.52637449	3.09001635	1.49500344	1.47708510
30	2.21654833	2.77783342	3.53280322	2.98566129	1.39097337	1.48314529
35	2.21681090	2.77765010	3.54044749	2.95043635	1.35607860	1.49042692
40	2.21704270	2.77746101	3.54913482	2.93006103	1.33601979	1.49877691
45	2.21736074	2.77737251	3.55990183	2.91630927	1.32258124	1.50922557
0.4	1.99405046	2.55373897	3.40012156	2.71826556	1.12501996	1.34942526
0.6	2.09290844	2.65210423	3.56535212	2.79772517	1.20486143	1.51427175
0.8	2.16201134	2.72293282	3.50814524	3.02941587	1.43521034	1.45840564
0.4+25	1.99343490	2.55515952	3.30382649	2.86908549	1.27408019	1.25453420
0.4+45	1.99419480	2.55419279	3.33701983	2.69261332	1.09889509	1.28633199
0.8+25	2.16200548	2.723732197	3.472249932	3.035338493	1.440330092	1.42295778
0.8+45	2.16303272	2.723041658	3.50570143	2.8619418	1.26821638	1.45502332

Absolute Error and Percentage Absolute Error Analysis

For the intraclass analysis, the feature vectors are utilized to calculate the Absolute Error (AE) and Percentage Absolute Error (PAE) as summarized in Tables 3 and 4. Table 3 indicates that LMI generally records smaller AE values in some cases, especially for minor rotations. However, KMI demonstrates greater consistency across both simple and complex transformations. Notably, Table 4 shows that KMI achieves lower PAE values under the 0.4 scaling factor and combined transformations (rotation + scaling), suggesting better generalization

Table III. Absolute Error

Moment invariant Technique	Image variation	Ø1	Ø2	Ø3	Ø4	Ø5	Ø6
KMI	25	0.049709	0.032262	0.065842	0.057118	0.074567	0.048397
LMI	25	0.000229	0.001025	0.051769	0.096501	0.095347	0.050973
KMI	0.4	0.407441	0.414049	0.316528	0.369834	0.363221	0.623138
LMI	0.4	0.222453	0.223241	0.178022	0.275249	0.274635	0.178633

Table IV. Percentage Absolute Error

Moment invariant Technique	Image variation	Ø1	Ø2	Ø3	Ø4	Ø5	Ø6
KMI	25	0.875541	0.577589	0.828253	0.722691	0.961311	0.635208
LMI	25	0.010362	0.036936	1.446833	3.223680	6.812211	3.335837
KMI	0.4	7.176382	7.412716	3.981721	4.679307	4.682557	8.178627
LMI	0.4	10.03624	8.038995	4.975280	9.194858	19.62168	11.69022

Percentage Mean Absolute Error (PMAE) Evaluation

Figure 3 graphically represents the Percentage Mean Absolute Error (PMAE) results. The LMI technique tends to produce higher PMAE values, particularly when scaling is introduced. This implies that LMI's feature extraction is more vulnerable to changes in image size and orientation. On the other hand, the KMI technique shows much smaller variations in PMAE, emphasizing its ability to maintain feature consistency under varied conditions.

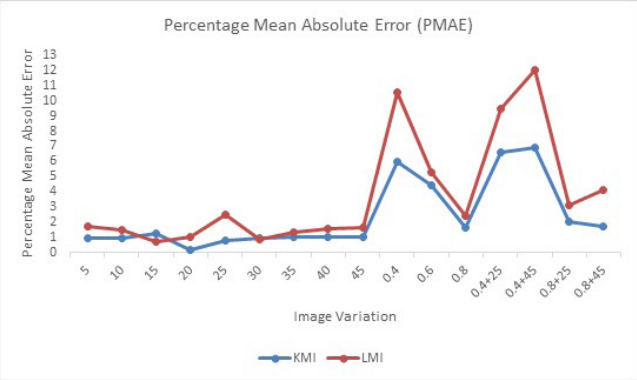

Figure 3: Percentage Mean Absolute Error (PMAE). This figure presents the PMAE values measured for different image variations, demonstrating how errors change when applying different transformations. It highlights that Legendre Moment Invariants (LMI) tend to produce higher errors compared to Krawtchouk Moment Invariants (KMI).

Total Percentage Mean Absolute Error (TPMAE) Comparison

Finally, Figure 4 presents the Total Percentage Mean Absolute Error (TPMAE) values for both techniques. TPMAE serves as an aggregate metric summarizing overall error behavior across all variations. KMI consistently records a significantly lower TPMAE than LMI. This confirms the earlier observations from individual AE and PAE values and further supports the conclusion that KMI is the more robust technique for invariant feature extraction.

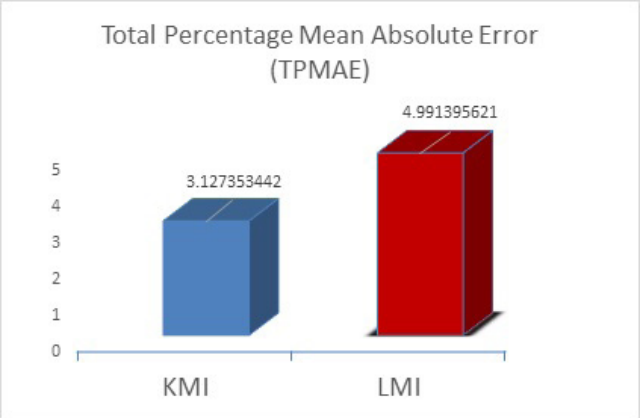

Figure 4: Total Percentage Mean Absolute Error (TPMAE). This figure visualizes the final stage of intra-class analysis, comparing the overall error rates for the two moment invariant techniques. It confirms that KMI yields the lowest TPMAE, indicating its superior performance in handling geometric transformations.

Summary of Findings

In addition to numerical results, the graphical presentations provide clear visual evidence of KMI's superiority. The flatter curve of KMI in both PMAE and TPMAE graphs highlights its reliability across multiple transformation scenarios. In practical terms, this implies that KMI-derived feature vectors are more likely to enable accurate recognition, classification, or retrieval tasks in medical imaging applications without being adversely affected by image distortions. Overall, the results demonstrate that although both techniques achieve invariance properties to a certain extent, Krawtchouk Moment Invariants perform more reliably and robustly under the geometric transformations evaluated. The ability to maintain low error rates in varied conditions positions KMI as a preferable choice for medical image feature extraction.

DISCUSSION

The results of this study provide important insights into the comparative performance of Legendre Moment Invariants (LMI) and Krawtchouk Moment Invariants (KMI) for feature extraction in medical images. A key finding is that KMI consistently demonstrated lower Percentage Mean Absolute Error (PMAE) and Total Percentage Mean Absolute Error (TPMAE) values compared to LMI, confirming its superior robustness under geometric transformations such as rotation, scaling, and their combinations.

The observed differences can be attributed to the fundamental nature of the two methods. LMI, despite its historical role and mathematical simplicity, depends heavily on global image properties. This makes it more sensitive to minor distortions, which explains the higher error values observed in this study, especially under complex transformations. These limitations are consistent with prior reports by Soon (6) and Machhour (15) where Legendre-based methods exhibited reduced stability under challenging imaging conditions.

By contrast, KMI is based on discrete orthogonal polynomials that emphasize localized intensity variations, enabling it to preserve features more effectively under distortions. This localized adaptability explains its consistently lower error values across transformation scenarios. Similar observations have been reported in other domains: Benouini (9) demonstrated the efficiency of KMI in 3D object classification, while Elouariachi (10) confirmed its robustness in sign language recognition. These findings collectively reinforce the strength of KMI in applications where feature stability under geometric variation is essential.

In the context of medical imaging, robustness to small but clinically meaningful variations is crucial. Even subtle differences in patient positioning, acquisition parameters, or equipment calibration can affect the reliability of computer-aided diagnostic (CAD) systems. Feature extraction techniques that remain stable under such variations can enhance downstream tasks such as disease classification, lesion detection, and image retrieval. The results of this study suggest that KMI holds greater potential than LMI in supporting these applications. Additionally, its relatively lower computational complexity compared to some advanced invariant techniques makes KMI suitable for real-time or high-throughput clinical environments.

The intraclass analysis framework used in this study further strengthens these findings by quantifying robustness with interpretable metrics (AE, PAE, PMAE, TPMAE). This practical evaluation approach simulates real-world distortions and highlights meaningful performance differences between the two methods. Moreover, KMI's mathematical design emphasizing localized feature capture suggests potential advantages in identifying subtle anomalies, such as faint opacities in chest radiographs, that global methods like LMI may fail to capture.

Despite these promising results, several limitations must be acknowledged. First, the evaluation was based on a single dataset (COVID-19 Radiography Database), and only one representative image was used for demonstration. This restricts the statistical validity of the findings. Second, the focus was limited to intraclass analysis, and interclass discrimination (e.g., distinguishing between normal and diseased states) was not examined. Finally, although LMI and KMI were compared here, other orthogonal moment families (Zernike, Tchebichef, Hahn, etc.) should also be included in future comparative studies to provide a more comprehensive benchmark.

Future work should therefore extend this analysis to larger and more diverse datasets, incorporate multiple imaging modalities such as CT and MRI, and include statistical testing to validate generalizability. Hybrid approaches that combine KMI with deep learning-based feature extraction may also offer a promising direction, leveraging the mathematical invariance of KMI with the adaptive learning capabilities of neural networks. Exploration of KMI in three-dimensional medical images represents another important avenue for future research.

In summary, while both methods demonstrate invariance properties, the findings of this study highlight the superior robustness, adaptability, and efficiency of KMI compared to LMI for feature extraction in medical imaging. These results position KMI as a strong candidate for integration into modern CAD systems, with the potential to enhance the reliability of diagnostic decision support tools.

CONCLUSION

This study presented a comparative evaluation of

Legendre Moment Invariants (LMI) and Krawtchouk Moment Invariants (KMI) for feature extraction in chest radiography images. Both techniques were capable of extracting invariant features under geometric transformations such as rotation, scaling, and combined distortions. However, intraclass analysis consistently showed that KMI achieved lower error values particularly lower TPMAE demonstrating superior robustness and adaptability compared to LMI. These findings suggest that KMI offers greater potential for reliable medical image feature extraction, especially in applications where stability under geometric variation is essential. Nonetheless, this work should be regarded as a proof-of-concept, as it was limited in dataset size and scope. Future research will focus on extending the analysis to larger and more diverse medical imaging datasets, incorporating statistical validation, and comparing additional moment invariant families. Hybrid approaches that integrate KMI with deep learning techniques and applications in three-dimensional imaging (CT, MRI) also represent promising directions for further investigation.

ACKNOWLEDGEMENTS

The author acknowledges to Universiti Malaysia Perlis (UniMAP) for the funding and support of the research work under Research Materials Fund (RESMATE), 9001-00627.

REFERENCES

1. Hu, M.K., 1962. Visual pattern recognition by moment invariants. IRE transactions on information theory, 8(2), pp.179-187. https://doi.org/10.1109/TIT.1962.1057692
2. Mukundan, R. and Ramakrishnan, K.R., 1998. Moment functions in image analysis: theory and applications. World scientific. https://doi.org/10.1142/3838
3. Teague, M.R., 1980. Image analysis via the general theory of moments. Josa, 70(8), pp.920-930. https://doi.org/10.1364/JOSA.70.000920
4. Yap, P.T., Paramesran, R. and Ong, S.H., 2003. Image analysis by Krawtchouk moments. IEEE Transactions on image processing, 12(11), pp.1367-1377. https://doi.org/10.1109/TIP.2003.818019
5. Aymaz, S., Aymaz, Ş. and Ulutaş, G., 2016, May. Detection of copy move forgery using Legendre moments. In 2016 24th signal processing and communication application conference (SIU) (pp. 1125-1128). IEEE. https://doi.org/10.1109/SIU.2016.7495942
6. Soon, F.C., Khaw, H.Y. and Chuah, J.H., 2015, December. Pattern recognition of vehicle logo using Tchebichef and Legendre moment. In 2015 IEEE Student Conference on Research and Development (SCOReD) (pp. 82-86). IEEE. https://doi.org/10.1109/SCORED.2015.7449438
7. Chiang, A. and Liao, S., 2017, June. Image analysis with symmetry properties of Legendre moments. In 2017 2nd International Conference on Image, Vision and Computing (ICIVC) (pp. 386-390). IEEE. https://doi.org/10.1109/ICIVC.2017.7984583
8. Dai, X., Shi, D. and Deng, H., 2016, July. Limited-view CT reconstruction based on discrete Krawtchouk moments. In 2016 3rd International Conference on Information Science and Control Engineering (ICISCE) (pp. 439-443). IEEE. https://doi.org/10.1109/ICISCE.2016.102
9. Benouini, R., Batioua, I., Zenkouar, K., Najah, S. and Qjidaa, H., 2018. Efficient 3D object classification by using direct Krawtchouk moment invariants. Multimedia tools and applications, 77, pp.27517-27542. https://doi.org/10.1007/s11042-018-5937-1
10. Elouariachi, I., Benouini, R., Zenkouar, K., Zarghili, A. and El Fadili, H., 2021, January. Explicit quaternion krawtchouk moment invariants for finger-spelling sign language recognition. In 2020 28th European Signal Processing Conference (EUSIPCO) (pp. 620-624). IEEE. https://doi.org/10.23919/Eusipco47968.2020.9287845
11. Yaakob, S.N., Saad, P. and Jamlos, M.F., 2006. On analysis of invariant characteristic for moment invariant techniques. Journal of Engineering.
12. Wafi, N.M., Yaakob, S.N., Salim, N.S., Jusoh, M., Nazren, A.R.A. and Hisham, M.B., 2016, October. Image analysis using new Descriptors Average Feature Optimization based on Fourier Descriptors technique. In 2016 International Conference on Radar, Antenna, Microwave, Electronics, and Telecommunications (ICRAMET) (pp. 135-138). IEEE. https://doi.org/10.1109/ICRAMET.2016.7849599
13. Nasrudin, M.W., Yaakob, S.N., Othman, R.R., Ismail, I., Jais, M.I. and Nasir, A.S.A., 2014, January. Analysis of geometric, Zernike and united moment invariants techniques based on intra-class evaluation. In 2014 5th international conference on intelligent systems, modelling and simulation (pp. 7-11). IEEE. https://doi.org/10.1109/ISMS.2014.9
14. Wafi, N.M., Sabri, N., Yaakob, S.N., Nasir, A.S., Nazren, A.R. and Hisham, M.B., 2017. Classification of Characters Using Multilayer Perceptron and Simplified Fuzzy ARTMAP Neural Networks. Advanced Science Letters, 23(6), pp.5151-5155. http://dx.doi.org/10.1166/asl.2017.7330
15. Machhour, A., Mallahi, M.E., Zouhri, A. and Chenouni, D., 2019, October. Image classification using shifted legendre-fourier moments and deep learning. In 2019 7th Mediterranean Congress of Telecommunications (CMT) (pp. 1-6). IEEE. https://doi.org/10.1109/CMT.2019.8931326